Electronic Supplementary Material (ESI) for Biomaterials Science.

Supplementary Information

Sustained release of drug-loaded nanoparticles from injectable hydrogels enables long-term control of macrophage phenotype

*Shreya S. Soni, Arielle M. D'Elia, Abdulrahman Alsasa, Sylvia Cho, Tina Tylek, Erin M. O'Brien, Ricardo Whitaker, Kara L. Spiller, and Christopher B. Rodell**

School of Biomedical Engineering, Science and Health Systems, Drexel University, Philadelphia, PA

*Corresponding author. Telephone: 215-895-2068; E-mail: christopher.b.rodell@drexel.edu

Table S1. Murine nanoString gene panel.

Gene	Target Identifier	Annotation
Acta2	NM_007392.2	ECM
Angpt2	NM_007426.3	Angiogenesis
Arg1	NM_007482.3	M2
Axl	NM_009465.4	M2
Bbgn	NM_007542.4	ECM
Birc3	NM_007464.3	M1
Ccl17	NM_011332.2	M2
Ccl2	NM_011333.3	M1
Ccl22	NM_009137.2	M2
Ccl4	NM_013652.1	M1
Ccl5	NM_013653.1	M1
Ccn2	NM_010217.2	ECM
Cd36	NM_007643.3	M1
Cd38	NM_007646.4	M1
Cd68	NM_009853.1	M1
Cd80	NM_009855.2	M1
Cd86	NM_019388.3	M1
Chil3	NM_009892.2	M2
Col1a1	NM_007742.3	ECM
Col6a1	NM_009933.2	ECM
Col3a1	NM_009930.1	ECM
Csf1r	NM_001037859.1	Immune signaling
Cxcl10	NM_021274.1	M1
Cxcl11	NM_019494.1	M1
Cxcl12	NM_021704.3	Immune signaling
Cxcr4	NM_009911.3	M1
Dcn	NM_001190451.1	ECM
Egr2	NM_010118.2	M2
Fn1	NM_010233.1	ECM
H2afx	NM_010436.2	M1
Igf1	NM_001111274.1	M2
Il10	NM_010548.2	M2
Il12b	NM_001303244.1	M1
Il1a	NM_010554.4	M1
Il1b	NM_008361.3	M1
Il6	NM_031168.1	M1
Irf3	NM_016849.4	M1
Irf4	NM_013674.1	M2
Irf5	NM_001252382.1	M1
Jak1	NM_146145.2	Immune signaling
Ki67	XM_006507413.5	M1
Mer	NM_008587.1	M2
Mmp13	NM_008607.1	Protease
Mmp14	NM_008608.3	Protease
Mmp2	NM_008610.2	Protease
Mmp8	NM_008611.4	Protease
Mmp9	NM_013599.2	Protease

Mrc1	NM_008625.1	M2
Nfkabia	NM_010907.2	M1
Nos2	NM_010927.3	M1
Pdgfb	NM_011057.3	Angiogenesis
S100a4	NM_011311.2	Fibrosis
Spp1	NM_009263.3	ECM
Stat3	NM_213659.2	M2
Stat6	NM_009284.2	M2
Tgfb1	NM_011577.1	M2
Timp1	NM_011593.2	ECM
Timp3	NM_011595.2	ECM
Tnf	NM_013693.2	M1
Top2a	NM_011623.2	M1
Vcan	NM_172955.1	ECM
Vegfa	NM_001025250.3	Angiogenesis
Vim	NM_011701.4	ECM
Hprt	NM_013556.2	Housekeeping
Tbp	NM_013684.3	Housekeeping

Table S2. Human nanoString gene panel.

Gene	**Target Identifier**	**Annotation**
Acta2	NM_001613.1:645	ECM
Aggf1	NM_018046.3:35	Angiogenesis
Ang	NM_001145.4:949	M2
Btg1	NM_001731.2:775	Immune signaling
Ccl15	NM_032965.4:869	Angiogenesis
Ccl18	NM_002988.2:585	M2
Ccl2	NM_002982.3:123	M1
Ccl22	NM_002990.3:797	M2
Ccl24	NM_002991.2:18	M2
Ccl26	NM_006072.4:184	M2
Ccl5	NM_002985.2:280	Angiogenesis
Ccl8	NM_005623.2:689	M1
Ccr7	NM_001838.2:1610	M1
Cd163	NM_004244.4:1630	M2
Cd80	NM_005191.3:674	M1
Clec10a	NM_182906.2:430	M2
Col3a1	NM_000090.3:180	ECM
Ctnnb1	NM_001098210.1:1815	Angiogenesis
Cxcr4	NM_003467.2:1335	Immune signaling
Egfl7	NM_016215.3:1252	Angiogenesis
Ets1	NM_005238.3:1305	Angiogenesis
Flt1	NM_002019.4:530	Angiogenesis
Fn1	NM_212482.1:1776	ECM
Foxo1	NM_002015.3:1526	Angiogenesis
Foxo4	NM_001170931.1:1121	Angiogenesis
Fyn	NM_002037.3:765	Immune signaling
Hspg1	NM_005529.5:2715	ECM

Ido1	NM_002164.5:369	M1
Il1b	NM_000576.2:840	M1
Il6	NM_000600.3:364	M1
Jag1	NM_000214.2:915	Immune signaling
Lum	NM_002345.3:1285	ECM
Marco	NM_006770.3:61	M2
Mmp2	NM_004530.2:2360	M1
Mmap9	NM_004994.2:1530	M2
Mrc1	NM_002438.2:525	M2
Pdgfa	NM_002607.5:2460	Angiogenesis
Pdgfb	NM_033016.2:1480	Angiogenesis
Pdgfc	NM_016205.2:2596	Angiogenesis
Pdgfra	NM_006206.3:1925	ECM
Pdgfrb	NM_002609.3:265	ECM
Ramp1	NM_005855.2:200	M2
Spp1	NM_000582.2:760	Immune signaling
Stat3	NM_003150.3:2060	Immune signaling
Stat6	NM_003153.3:2030	Immune signaling
Tgfb1	NM_000660.3:1260	ECM
Tie1	NM_005424.2:2610	Angiogenesis
Timp3	NM_000362.4:1640	Immune signaling
Tnf	NM_000594.2:1010	M1
Tnfrsf11a	NM_003839.3:226	M2
Vcan	NM_004385.3:9915	ECM
Vegfa	NM_001025366.1:1325	Angiogenesis
Vegfb	NM_003377.3:687	Angiogenesis
Vegfc	NM_005429.2:565	Angiogenesis
Vim	NM_003380.2:694	ECM
Wnt5a	NM_003392.3:475	Immune signaling
Gapdh	NM_001256799.1:386	Housekeeping
Tbp	NM_001172085.1:587	Housekeeping

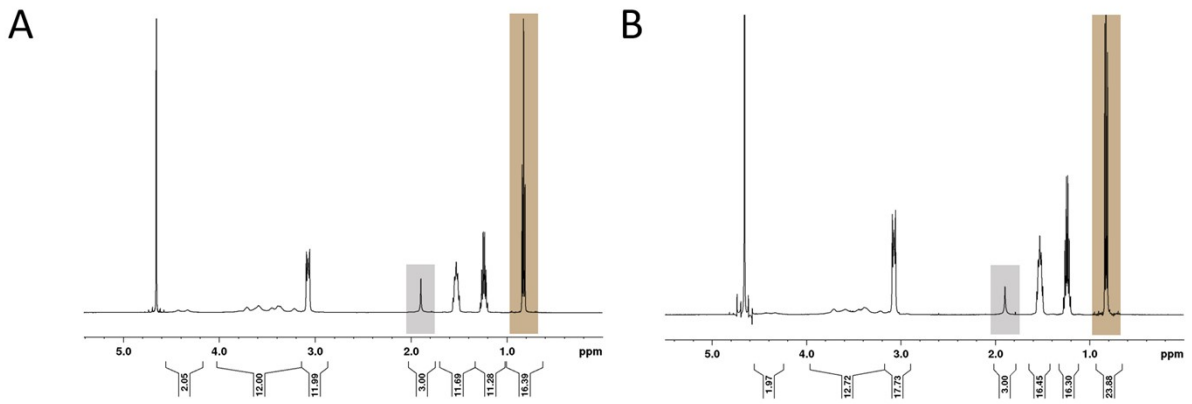

Figure S1. [1]H-NMR spectra of the tetrabutylammonium salt of **(A)** 82 kDa and **(B)** 337 kDa hyaluronic acid (HA-TBA). The ratio of TBA to HA repeat units is determined by the integration of the TBA methyl group (12H, shaded brown) relative to the N-acetyl group of HA (3H, shaded gray).

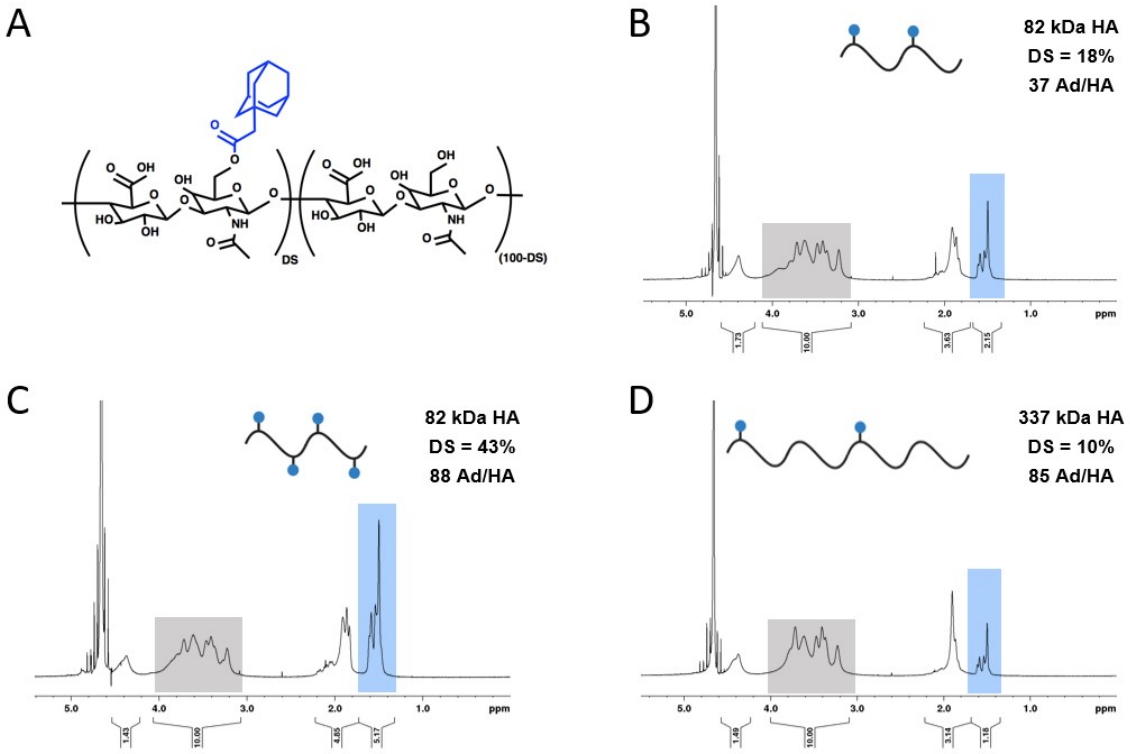

Figure S2. A) Chemical structure of adamantane functionalized hyaluronic acid (Ad-HA). **B-D)** [1]H-NMR spectra of Ad-HA products. The degree of substitution (DS) is determined by integration of the ethyl multiplet of adamantane (12H, shaded blue) relative to the sugar ring of HA (10H, shaded gray). For low molecular weight HA **(**82 kDa), a DS of 18% **(B)** and 43% (**C**) yield an average of 37 and 88 Ad per HA macromer, respectively. For high molecular weight HA (337 kDa), a DS of 10% afforded a calculated average of 85 guest groups per macromer.

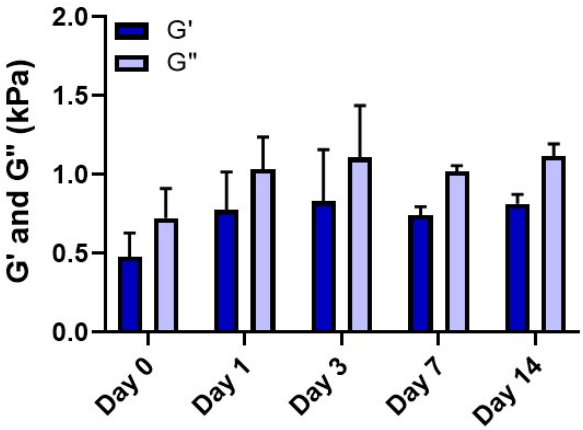

Figure S3. Temporal dependence of rheological properties of hydrogels composed of 82 kDa Ad-HA (Low), 1:1 ratio Ad-HA:CDNP. Time sweeps were performed at 10.0 Hz, 1.0% strain; G' (dark blue), G" (light blue); mean ± SD, n = 2.

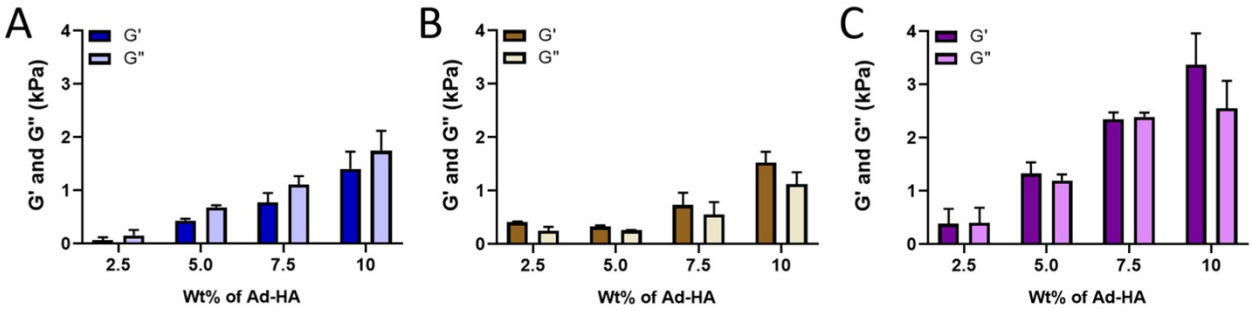

Figure S4. Storage (G', darker shading) and loss (G'', lighter shading) moduli of **A)** 82 kDa Ad-HA (Low), 1:1 ratio Ad-HA:CDNP, **B)** 337 kDa Ad-HA (Low), 1:0.5 ratio Ad-HA:CDNP, and **C)** 82 kDa Ad-HA (High), 1:1.5 ratio Ad-HA:CDNP dependent on the concentration of Ad-HA. Time sweeps were performed at 10.0 Hz, 1.0% strain; mean ± SD, n = 2.

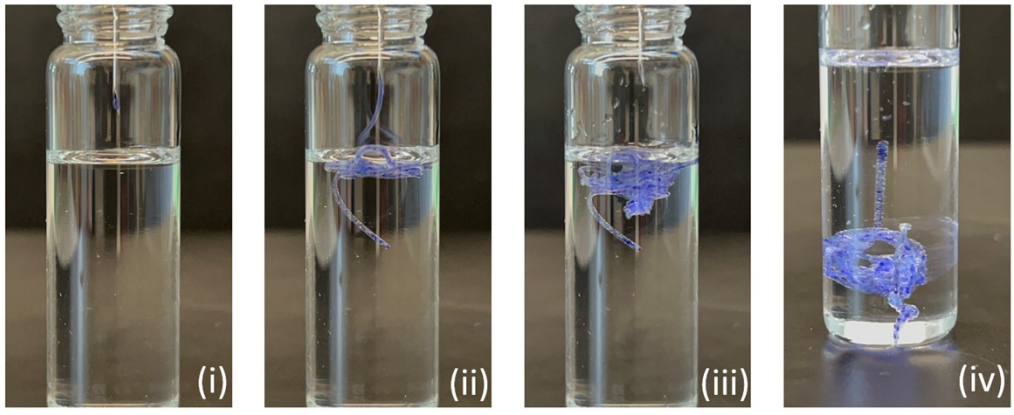

Figure S5. Representative images of shear-thinning hydrogel injection through a 21G needle fitted to a 1 mL syringe.

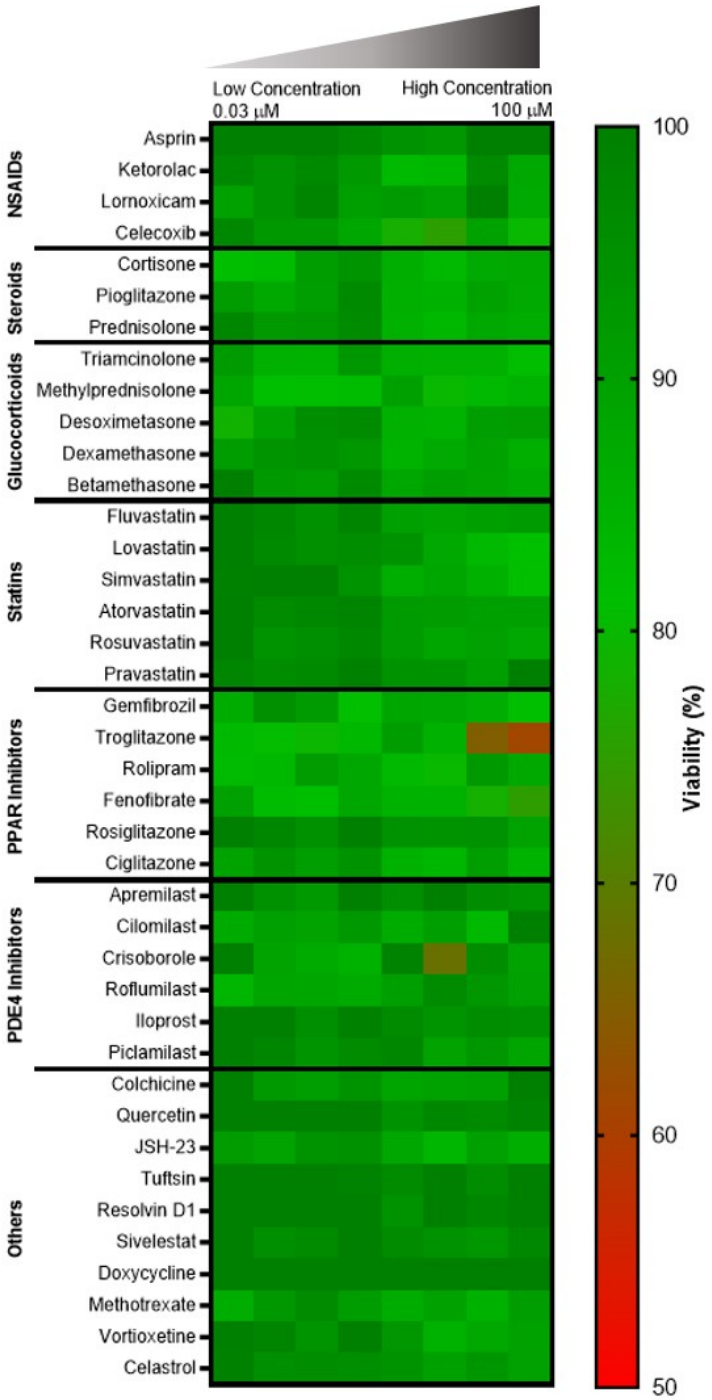

Figure S6. Cytotoxicity assessment of drug compounds. RAW264.7 cells were treated with indicated drug, spanning a dose-response from 100 μM to 31.6 nM in half-log titration. Heat map represents cell viability, as determined by PrestoBlue™ following normalization to untreated control wells. Data represent the mean of n = 3 independent samples.

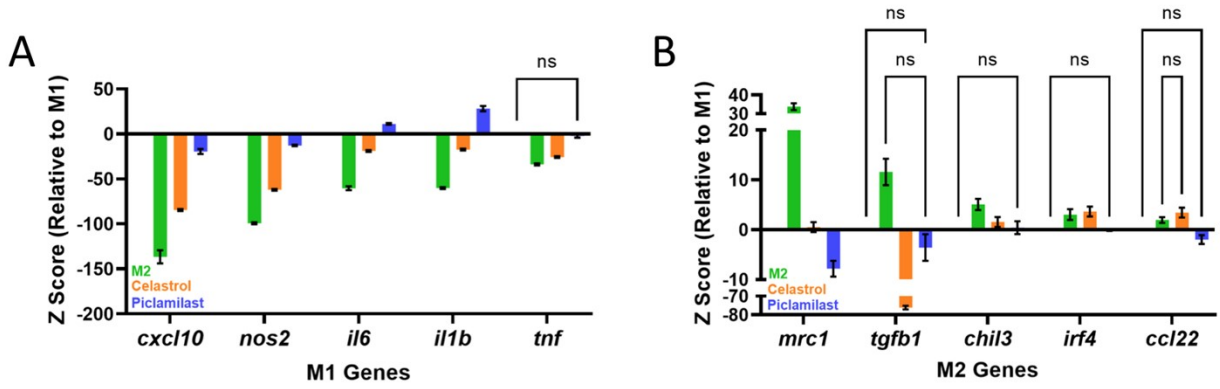

Figure S7. Expression of M1-associated **(A)** and M2-associated **(B)** genes following treatment by celastrol (orange) or piclamilast (blue) in BMDMs. M2 controls (green) are included for reference; $p < 0.05$ for all comparisons unless indicated (ns = not significant). Results represent the group Z-score relative to M1-like controls; mean ± SD, n = 3.

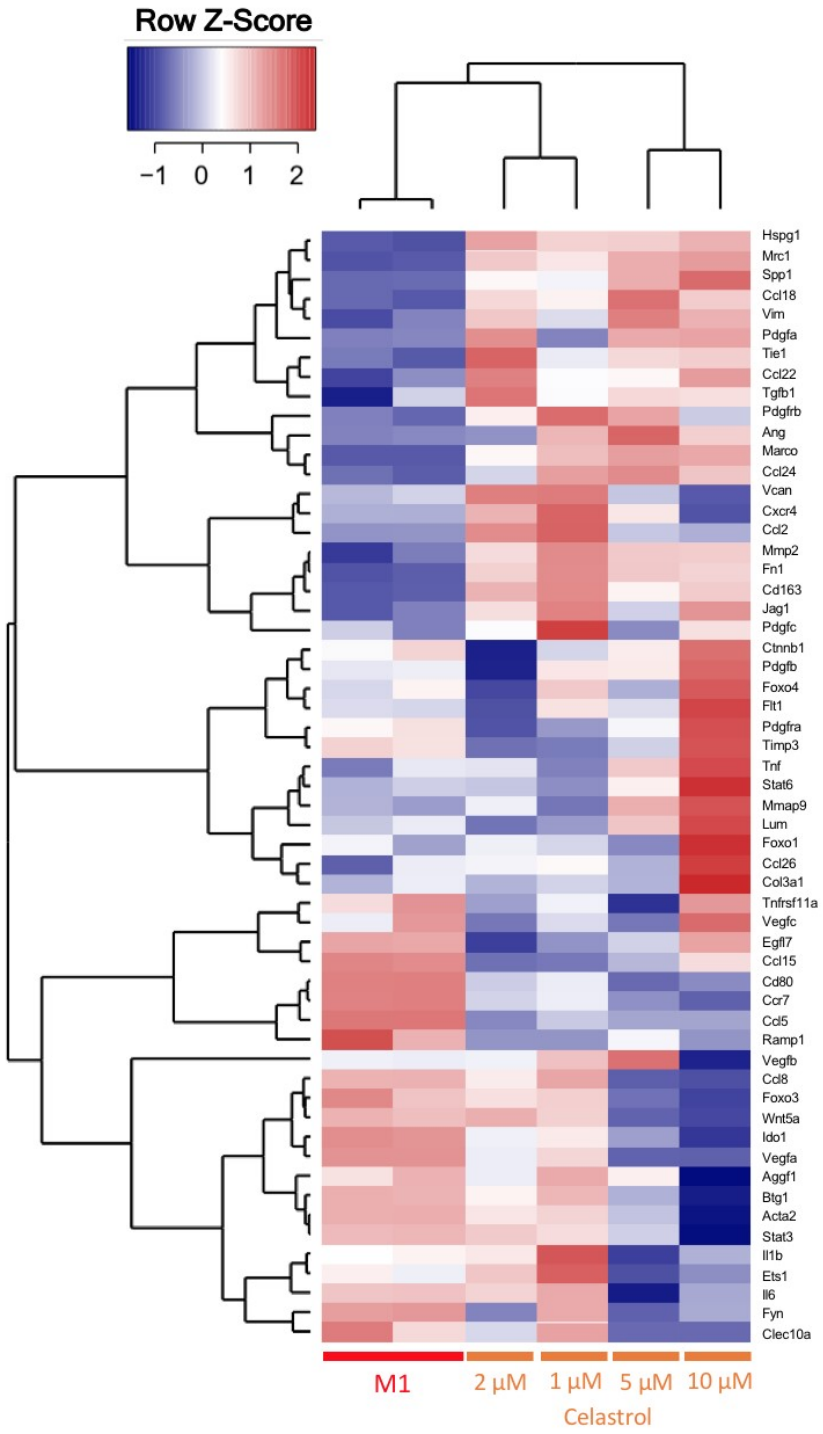

Figure S8. Heatmap of expressed genes represented as the row Z-score of log-transformed normalized data. Genes that were not expressed above background are excluded from presentation. Human monocyte-derived MF were subject to celastrol treatment at varying doses concurrent with LPS activation (100 ng/mL). M1 controls are included for reference. Low (1, 2 μM) doses clustered similarly, while higher doses (5, 10 μM) further diverged from M1 transcriptional profiles.

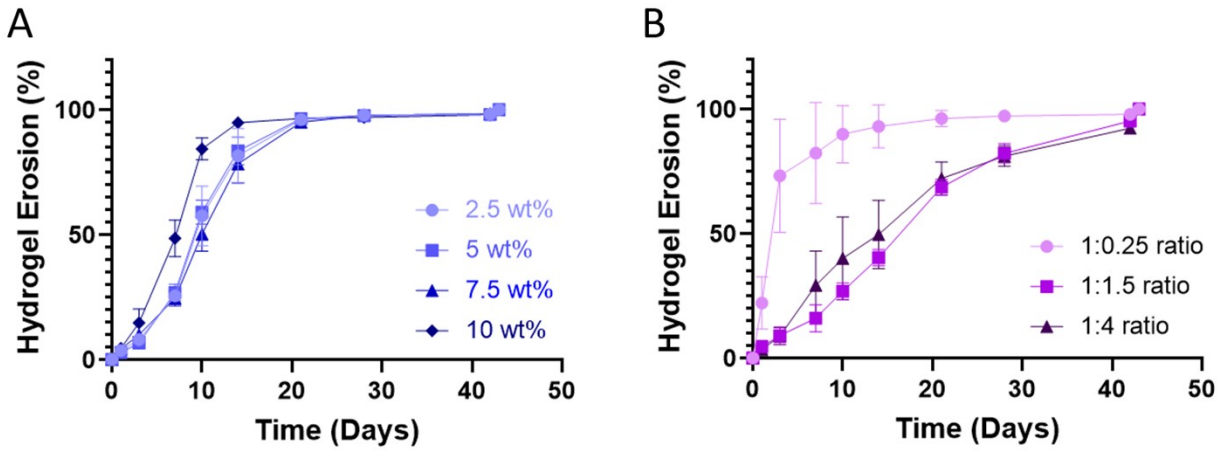

Figure S9. Hydrogel erosion is dependent on polymer concentration and the ratio of guest-to-host components. Hydrogel erosion occurred over a period of greater than one month, with minimal dependence on polymer concentration (**A**; 82 kDa Ad-HA (Low); 2.5-10%$_{w/v}$) and a more pronounced dependence on the volumetric ratio of Ad-HA-to-CDNP (**B;** 82 kDa Ad-HA (High); 1:0.25-1:4 ratio). Data represent the mean ± SD, n = 4.

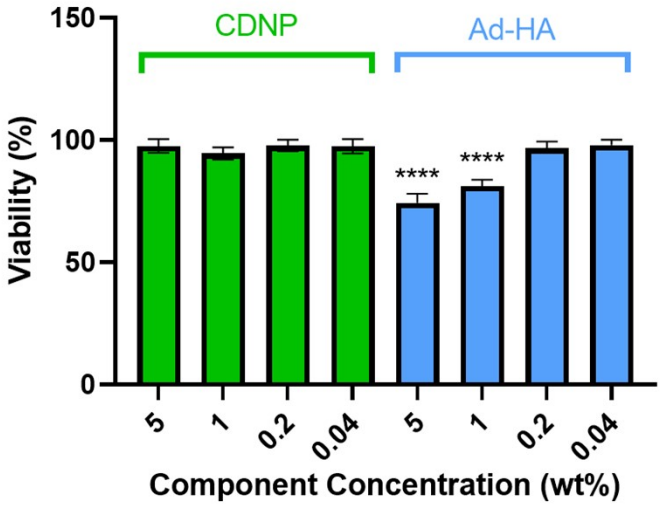

Figure S10. Cell viability in response to guest and host hydrogel components. Cells were assessed by PrestoBlue™ after 24 hrs of exposure to the individual components (CDNP or 82 kDa Ad-HA (High)) dissolved in media at varying concentrations. Data represent the mean ± SD, n = 3, ****p value < 0.0001 relative to untreated controls.

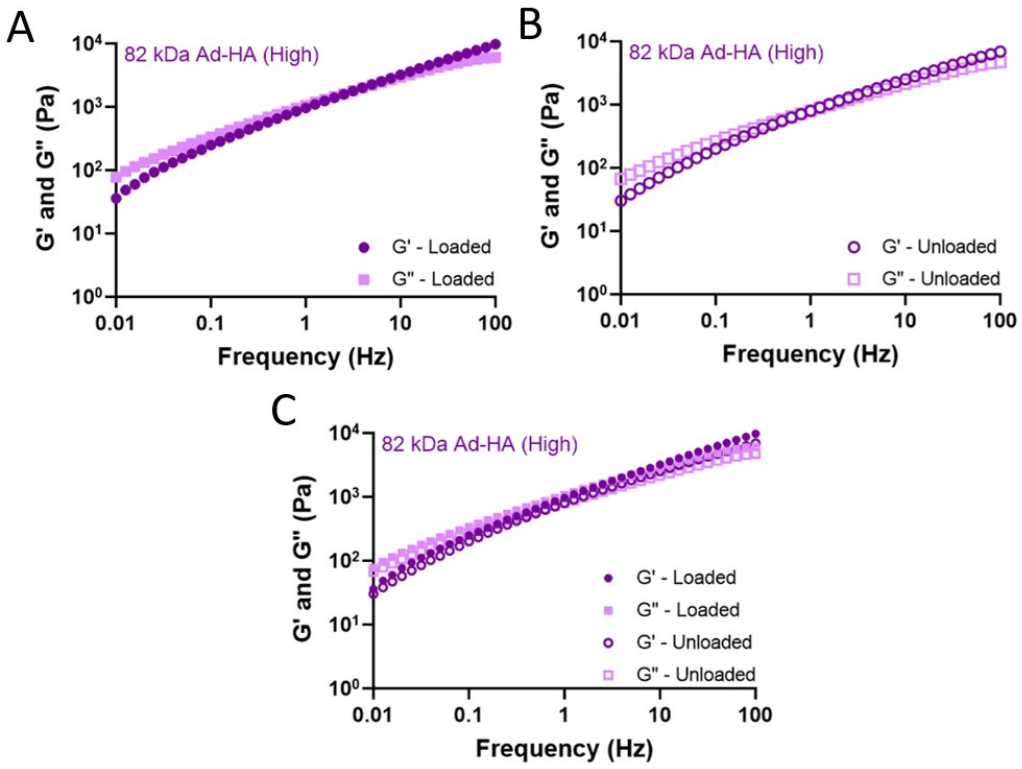

Figure S11. Representative oscillatory frequency sweeps of drug loaded (**A**, closed symbol) and unloaded (**B**, open symbol) hydrogels, and overlaid response (**C**) for 82 kDa Ad-HA (High) at a 1:1.5 Ad-HA:CDNP ratio; G' (dark purple), G" (light purple).

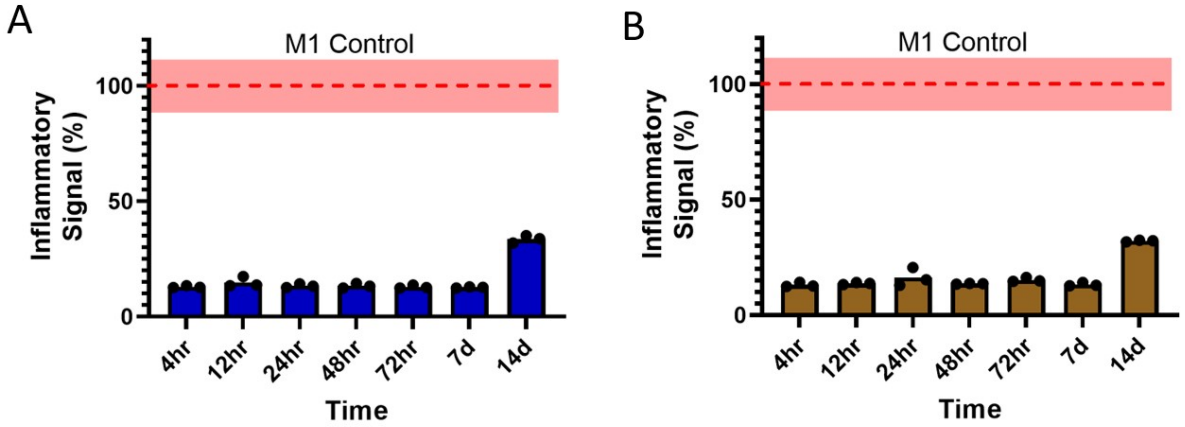

Figure S12. Anti-inflammatory activity of drug release samples performed in RAW-Blue™ cells by concurrent zymosan stimulation (100 µg/mL) and treatment with conditioned media from **(A)** 82 kDa Ad-HA (Low) and **(B)** 337 kDa Ad-HA (Low) hydrogels; p value < 0.0001 for all samples relative to zymosan-treated controls (dashed line, red). Data represent the mean ± SD, n = 3.

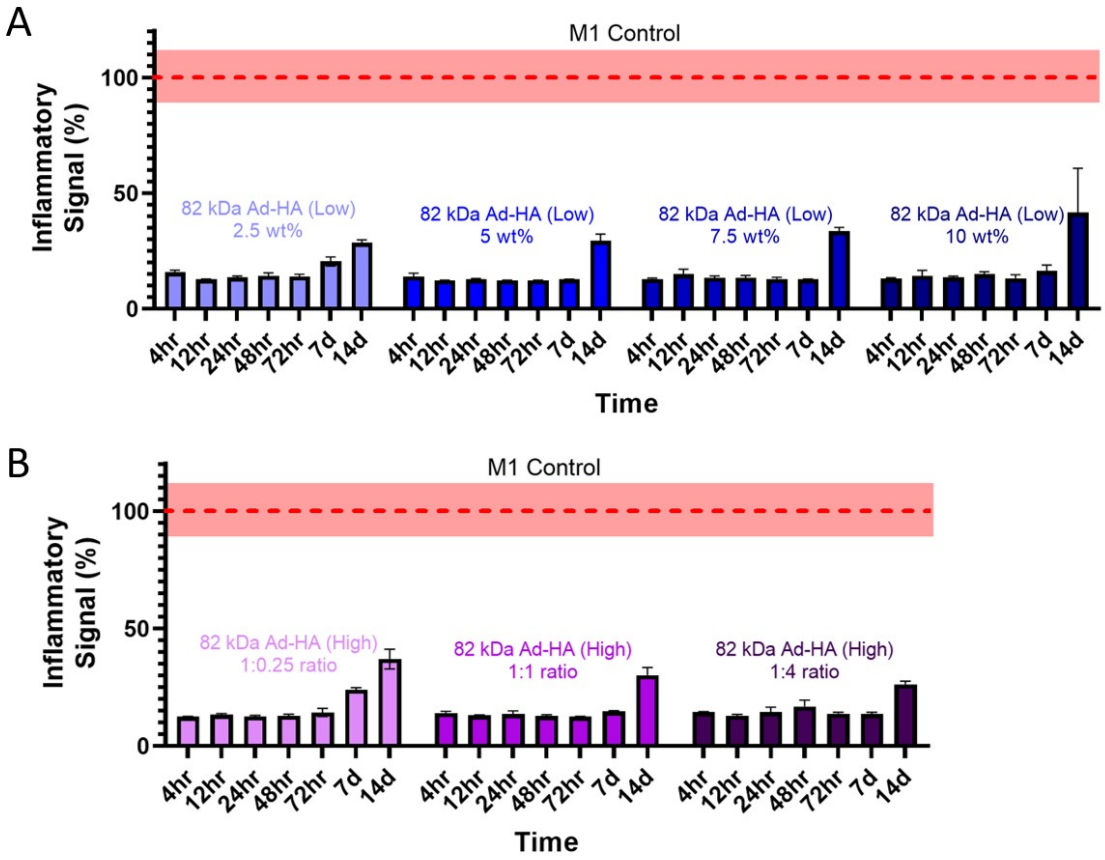

Figure S13. Anti-inflammatory activity of drug release samples performed in RAW-Blue™ cells by concurrent zymosan stimulation (100 µg/mL) and treatment with conditioned media from **(A)** 82 kDa Ad-HA (Low) hydrogels at varying concentrations of Ad-HA and (**B)** 82 kDa Ad-HA (High) hydrogels at varying ratios of Ad-HA:CDNP; p value < 0.0001 for all samples relative to zymosan-treated controls (dashed line, red). Data represent the mean ± SD, n = 3.